Available online at www.sciencedirect.com

SciVerse ScienceDirect

Physics Procedia 35 (2012) 4 – 9

Physics Procedia

Positron Studies of Defects 2011

Microstructure development and lateral distribution of defects in ultra-fine grained copper prepared by high-pressure torsion

Ivan Procházka [a,*], Jakub Čížek [a], Oksana Melikhova [a], Zuzana Barnovská [a], Miloš Janeček [b], Ondřej Srba [b], Radomír Kužel [c], Sergej V. Dobatkin [d]

[a] *Charles University in Prague, Faculty of Mathematics and Physics, Department of Low Temperature Physics, V Holešovičkách 2, CZ-180 00 Praha 8, Czech Republic*

[b] *Charles University in Prague, Faculty of Mathematics and Physics, Department of Physics of Materials, Ke Karlovu 5, CZ-121 16 Praha 2, Czech Republic*

[c] *Charles University in Prague, Faculty of Mathematics and Physics, Department of Condensed Matter Physics, Ke Karlovu 5, CZ-121 16 Praha 2, Czech Republic*

[d] *A.A. Baikov Institute of Metallurgy and Materials Science, Russian Academy of Sciences, Leninskii pr. 49, Moscow 119991, Russia*

Abstract

A defect study of ultra-fine grained (UFG) Cu prepared by high-pressure torsion (HPT) will be reported. Conventional positron annihilation spectroscopy (PAS) including positron lifetime (PLT) and Doppler broadening (DB) techniques was employed as the main experimental tool. PAS was combined with transmission electron microscopy, X-ray diffraction and Vickers microhardness (HV) measurements. First, lattice defects introduced by HPT were characterized. A very high concentration of defects created during HPT deformation was observed and the two kinds of defects could be identified: dislocations and small vacancy clusters (microvoids). Further investigations were focused on (i) the radial distributions of defects and (ii) the evolution of microstructure during HPT processing. The results of the present study are consistent with an increase of shear strain from the sample centre toward its periphery. Extended lateral mapping of microstructure was performed using HV and DB techniques. The latter one reveals a significant non-uniformity of defect distribution which was less pronounced in the HV measurements.

Keywords: Ultra-fine grained copper; high-pressure torsion; lateral distribution of defects; dislocations; microvoids; positron annihilation spectroscopy.

1. Introduction

Materials with mean grain size reduced down to several hundreds of nanometers are referred to as the ultra-fine grained (UFG) materials. Grain refinement of ordinary polycrystalline materials often brings an improvement of

* Corresponding author. Tel.: +420-221 912 769; fax: +420-221 912 567.
E-mail address: ivan.prochazka@mff.cuni.cz.

1875-3892 © 2012 The Authors Published by Elsevier B.V. Selection and/or peer-review under responsibility of Organizing Committee.
doi:10.1016/j.phpro.2012.06.002

their mechanical properties, for example, a high strength combined with a reasonable ductility [1]. Grain boundaries (GB's) become to play a substantial role in UFG materials and obviously assist e.g. to an increase of diffusion activity of atoms [2] and ductility [3]. A remarkable grain refinement can be attained by the techniques based on severe plastic deformation [1], e.g. by the high-pressure torsion (HPT). The HPT deformation is performed by placing a material between two anvils and straining it by the rotating anvil under a uniaxial pressure of several GPa. In many metals or metallic alloys, grain refinement to a typical grain size of ≈ 100 nm is achieved by means of HPT treatment [1]. Among such materials, UFG copper is a good model system for comparative studies of different preparation techniques because pure copper is easily accessible and various characterization methods are applicable.

HPT treatment results in disk-shaped bulk specimens having typically a diameter of 10 – 15 mm and a thickness of ≈ 0.3 mm. A huge amount of lattice defects (vacancies, dislocations) is created during HPT deformation. It can be anticipated, that the HPT imposed shear strain is raised proportionally to the radial distance from the disk centre and to the number of torsion turns [1]. Consequently, the microstructure at the disk centre can expected to differ from that at the disk edge. Such a microstructure pattern was supported by a lower hardness at the disk centre compared to its periphery measured on HPT deformed Ni [4]. On the other hand, the microstructure differences between the sample periphery and its centre were indicated to become smaller under a higher pressure applied during HPT deformation and with an increasing number of turns [5]. Hence, a detailed knowledge of the microstructure variations in dependence on preparation conditions, in particular the type and spatial distribution of defects induced during HPT processing, is obviously a key issue in attempts to understand unusual properties of HPT deformed materials and to optimize material preparation procedure.

In the present Contribution, a detailed defect study of UFG Cu prepared by HPT was performed. The Contribution is focused on (i) the characterization of defects introduced by HPT, (ii) the lateral distribution of defects and (iii) the microstructure evolution during HPT processing. Conventional positron annihilation spectroscopy (PAS) combined with X-ray diffraction (XRD), transmission electron microscopy (TEM) and Vickers microhardness (HV) measurements were involved [6,7].

2. Experimental

Copper of 99.95 % purity was HPT deformed at room temperature. A series of samples subjected to 1, 3, 5 10, 15 and 25 revolutions were investigated in order to follow the evolution of microstructure during HPT treatment. A possible effect of compressive pressure was also studied using samples deformed under 2 and 4 GPa. HPT processing resulted in disk-shaped specimens having a diameter of ≈ 9 mm and a thickness of ≈ 0.3 mm.

HV measurements were performed using a STRUERS Duramin 300 hardness tester with a load of 100 g applied for 10 s. HPT deformed Cu samples were polished to a mirror-like quality for HV investigations. The homogeneity of microstructure was characterized by HV measured on a rectangular $x - y$ grid with the incremental spacing of 0.5 mm. Colour coded maps of HV results were constructed to provide pictorial displays about the homogeneity of microstructure across the sample.

Two positron sources, made of carrier-free ^{22}Na carbonate salt (iThembaLABS) deposited and sealed between two 2 μm thick mylar C foils (Dupont), were used: (I) a stronger source, having ≈ 1 MBq strength and an activity spot of ≈ 3 mm diameter, and (II) a weaker source (≈ 0.5 MBq strength, < 1 mm spot size). Positron source was sandwiched between two identical disks of the material studied.

Positron lifetime (PLT) measurements were performed using the source (I) and a fast-fast PLT spectrometer similar to that of Ref. [8]. The spectrometer exhibited a time resolution of 150 ps (FWHM) and a coincidence count rate of ≈ 100 s^{-1} for the above positron source. Positron annihilations in the source and its cover foils contributed to measured PLT spectra with the two weak components exhibiting lifetimes (intensities) of 0.368 ns (8 %) and 1.5 ns (1 %). These components were extracted based on PLT measurements with the well-annealed Cu reference material. Radial variations of microstructure were investigated by making PLT measurements with the positron source positioned at the sample centre (i.e. at a radial distance of $r \approx 0$) and at a periphery position ($r \approx 3$ mm).

Doppler broadening (DB) experiments were carried out using the weaker source (II) and an ordinary HPGe γ-ray spectrometer having an energy resolution of 1.3 keV (FWHM) at the 511 keV γ-ray energy. Doppler profiles were described in terms of the ordinary sharpness and wing parameters, S and W, respectively, normalised to the shape parameters measured at the centre of the sample after one HPT revolution (S_0 and W_0, respectively). The lateral variations of microstructure were mapped in detail using DB measurements performed for different source positions

incremented in 1 mm steps along a rectangular grid. Source positions were adjusted by means of a micrometer $x - y$ shift with a precision of ≈ 0.1 mm.

3. Results and discussion

3.1 Basic information coming from TEM and XRD

TEM observations on HPT deformed Cu revealed already after 1 turn a heavily deformed structure with a high dislocation density over the whole sample with typical features of initial stages of dislocation rearrangement at the sample centre and a more refined microstructure at the sample periphery [6]. TEM images obtained for the sample subjected to 15 revolutions and 4 GPa pressure indicated that grain refinement to a mean grain size of 200 – 300 nm is achieved at the sample periphery, but differences between the sample centre and its periphery still persist: dislocation cells plus subgrains separated by tangled dislocations are seen by TEM in the central region [6].

XRD experiments on HPT deformed Cu showed [6] the mean size of coherently scattering domains to become as low as ≈ 100 nm already after the first turn. Note that the domain size determined from XRD is always smaller than the grain size estimated by TEM. This is because XRD provides a mean size of coherently diffracting crystallites with almost perfect structure free of microstrains (e.g. dislocation cells and subgrains) while the grains separated by well-defined GB's are discerned by TEM. Starting from the third turn, the coherent domain size is not diminished more, remains roughly constant with increasing number of turns and appears to be slightly smaller for the 4 GPa applied pressure compared to that of 2 GPa (≈ 50 and ≈ 70 nm, respectively). A high dislocation density averaged over the sample, $\rho_D \approx 7\times10^{15}$ m^{-2}, could be deduced from the line profile analysis. Only a very slight increase of the mean dislocation density with number of HPT turns and no significant variations of ρ_D with applied pressure were indicated, see Ref. [6].

3.2 PLT experiments

In PLT spectra measured on HPT deformed copper, two exponential components were resolved (lifetimes τ_i , intensities I_i , i = 1,2) except for the positron source contribution. In Fig. 1a, observed lifetimes τ_1 , τ_2 were plotted as functions of the number of HPT revolutions for the two pressures used, 2 and 4 GPa, and the two positions of the positron source, central ($r \approx 0$) and peripheral ($r \approx 3$ mm) ones. Similarly, measured intensities I_2 are represented in Fig. 1b. The positron lifetimes of Fig. 1a were found to be substantially higher than the lifetime $\tau_b = 114$ ps reported [10] for the well-annealed Cu reference material. Thus, undoubtedly, both observed lifetimes originate from positron trapping in defects. Lifetimes τ_1 appear to be close to a value of 164 ps which is known as the lifetime of positrons trapped at dislocations [10]. Thus, the τ_1-component which dominates PLT spectra of HPT deformed Cu arises from positron trapping at the dislocations created during severe plastic deformation. The longer component (lifetime τ_2) comes from positron trapping in the larger defects (microvoids) of open volume equivalent to a cluster of several vacancies. Comparing the experimental τ_2-values with those calculated in Ref. [9], the size of clusters could be estimated as 4 – 5 vacancies at the sample centre and 7 – 9 vacancies at the sample periphery. The estimated size intervals cover also a non-statistical scatter, seen in Fig. 1 a, which may result from a possible small variations of sample preparation conditions. It can be seen in Fig. 1 that the number of HPT revolutions does not influence significantly cluster size. A well-pronounced effect of positron trapping in vacancy clusters can be regarded as

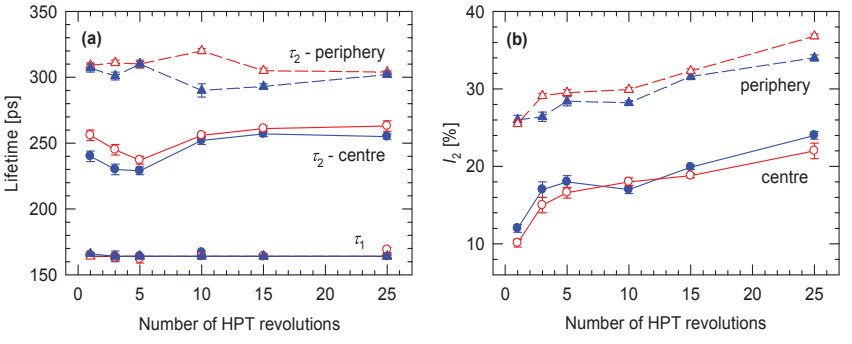

Fig. 1. Results of PLT investigations plotted as a function of the number of HPT revolutions: (a) lifetimes of exponential components resolved in PLT spectra, (b) relative intensity I_2 (I_1 + I_2 = 100%) of the contribution of positrons trapped in vacancy clusters. Results of measurements taken at the centre of the sample ($r \approx 0$ mm) are plotted by circles while those performed at the periphery ($r \approx 3$ mm) are plotted by triangles. Data obtained on samples deformed under the pressure of 2 and 4 GPa are plotted by full and open symbols, respectively. Error bars include statistical noise contribution only.

a strong evidence of a high number of vacancies formed by HPT deformation in Cu [6]. These vacancies are mobile at room temperature and, hence, they either disappear via diffusion to sinks or aggregate into small clusters. The I_2-data in Fig. 2 b suggest that either the microvoids concentration in the sample centre is lower than in its periphery or the trapping rate is enlarged due to a larger defect size in the periphery.

3.3 HV mapping

Fig. 2 shows colour coded maps of HV distributions across the sample subjected to various numbers of HPT revolutions, N, under 4 GPa pressure. The sample subjected to one HPT revolution exhibits a lowered HV ≈ 116 in the centre while the periphery is characterized by a high HV ≈ 150. With an increasing number of HPT revolutions, HV in the centre increases and the differences in HV values between the central and the periphery regions become smaller. Obviously, a high HV at the periphery, seen already after the first HPT revolution, is caused by the fact that this region is subjected to the highest strain. With an increasing number of HPT turns, the region characterized by high HV's extends gradually toward the centre. The sample subjected to 25 HPT turns exhibits almost uniform HV everywhere at a distance $r > 1$ mm. However, its centre is still characterized by a slightly lower HV.

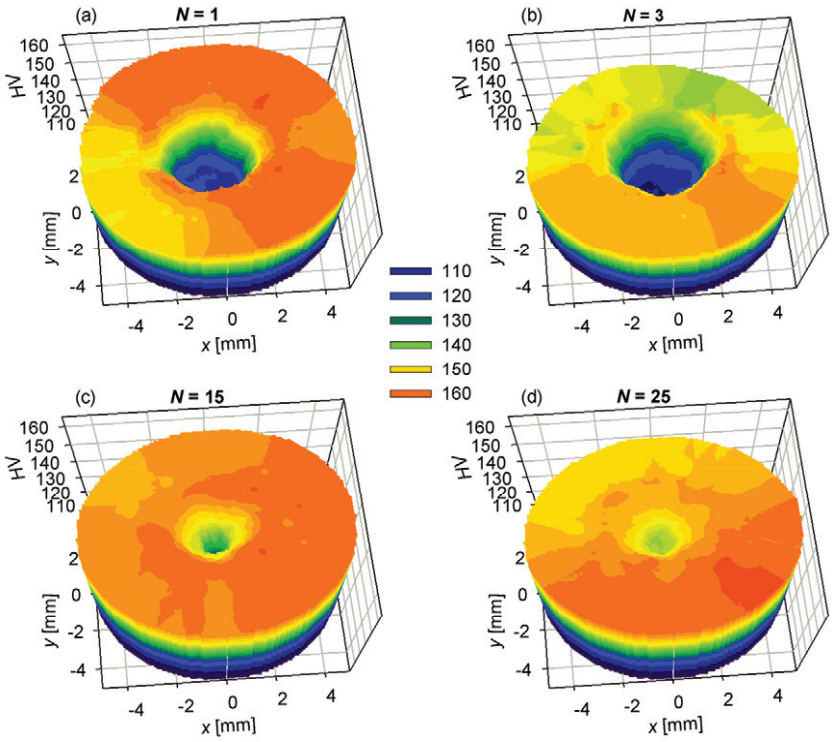

Fig. 2. Colour coded map constructed from HV values measured on a rectangular $x - y$ grid (incremental spacing 0.5 mm) for HPT deformed Cu subjected to N=1, 3, 15 and 25 revolutions.

3.4 DB mapping

The lateral distribution of defects in HPT deformed Cu was mapped for samples subjected to 1, 3, 15 and 25 turns under 4 GPa pressure. Fig. 3 shows colour coded maps constructed from the S parameter values. The Figure illustrates a radial symmetry of defect distribution (dislocations and microvoids) over the disk plain. The radial dependences of S parameter are plotted in Fig. 4a. Fig. 4b shows the data arranged into the S–W plot.

The most pronounced feature revealed by DB measurements is an increase in S parameter (and corresponding decrease in W parameter) from the sample centre toward its edge. Note that no significant variations of dislocation density are indicated by XRD measurements on HPT deformed Cu [6]. Then the observed radial changes of S and W parameters should obviously be attributed to an enlarged size of vacancy clusters at the sample periphery compared to its centre, as suggested also by the PLT measurements (7 – 9 compared to 4 – 5 vacancies, respectively). Not only the S parameter for positrons trapped in microvoids but also the trapping rate (i.e. the

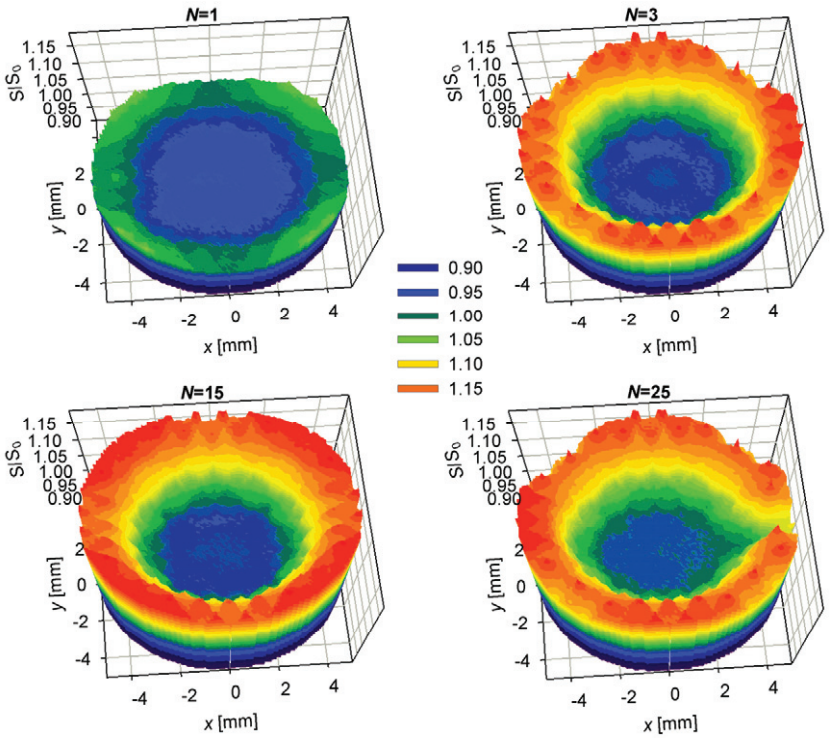

Fig. 3. Colour coded map constructed from S values measured on a rectangular $x - y$ grid (incremental spacing 1 mm) for HPT deformed Cu subjected to N=1, 3, 15 and 25 revolutions.

positron fraction) to microvoids is increased at the sample periphery. Correspondingly, a decrease of W values accompanying an increase of S values at the sample periphery is understood. An amount of defects introduced by HPT deformation is increased with increasing the number of turns what is reflected by a general trend of a growth of S- and a drop of W-values seen in Fig. 4a. Similarly to PLT results this effect is pronounced for lower number of turns. It can be read from the S–W plot on Fig. 4b that S and W values are arranged roughly along a straight line which testifies that the nature of positron traps does not change substantially but the defect concentration does. With increasing radial distance, S is increased and W decreased which results in a negative slope of the plot. Radial variations in size of vacancy clusters cause an increase of trapping rate as well as a growth of S and, correspondingly, a drop of W. This is likely a reason for small but systematic deviations from linearity of the data plotted in Fig. 4b.

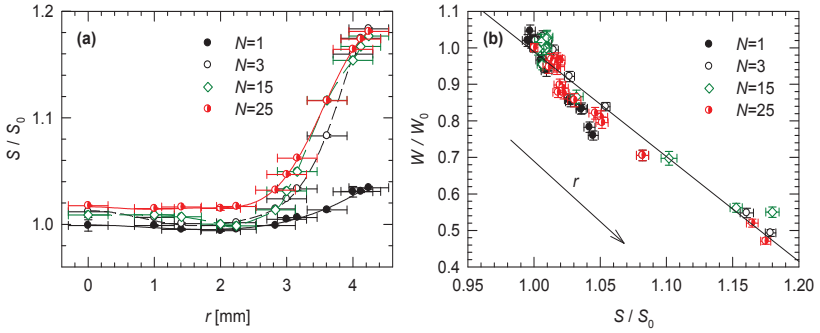

Fig. 4. (a) The dependence of the S parameter on the radial distance r from the sample centre. Each data point in the panel is an averaged value over all nodes of the rectangular grid with the same distance from the centre. (b) The S-W plot constructed from the S and W values of panel (a). The error bars of the radial distance account for a finite source size, while those of S and W parameters include statistical noise only. The straight line in panel (b) is a linear fit to all points of the panel. The arrow in panel (b) points in the direction of increasing r. N denotes the number of HPT revolutions.

One can note that general trends displayed by HV and S parameter mapping are similar as they reflect increasing defect densities and decreasing grain size due to a higher imposed strain. However, HV is influenced by grain size and dislocation density, while DB conveys information on deformation induced vacancies which have a relatively low impact on hardness, but influence other physical

properties of the UFG material (diffusion, phase transformations etc.). Hence, both methods of mapping are complementary, since they respond to different aspects of microstructure.

4. Conclusions

The two kinds of lattice defects could be resolved by PLT measurements in HPT deformed Cu – dislocations and small vacancy clusters formed by agglomeration of deformation-induced vacancies. Microstructural inhomogeneity of HPT deformed Cu was characterized by HV and DB mapping. It was demonstrated that DB mapping carries information about spatial distribution of dislocations and vacancy clusters. Hence, DB technique should be considered as a valuable tool complementary to the standard HV characterization. It was found that the *S* parameter strongly increases with the radial distance from the centre due to increasing size of vacancy clusters. Although HV mapping showed only a slight difference between the centre and the periphery in the sample subjected to 25 HPT revolutions, DB mapping revealed that lateral distribution of vacancy clusters is still far from being uniform.

Acknowledgement

This work was supported by the Academy of Sciences of the Czech Republic (under projects KAN 300100801 and IAA 101120803) and by the Ministry of Education, Youths and Sports of the Czech Republic (scientific plan MSM 0020821634). Partial support from Charles University within project SVV-2010-261303 is also acknowledged.

References

[1] R.Z. Valiev, R.K. Islamgaliev, I.V. Aleksandrov, Prog. Mater. Sci. 45 (2000) 103.
[2] R.Z. Valiev, R.Sh. Musalimov, N.K. Tsenev, Phys. Status Solidi (a) 115 (1989) 451.
[3] R.Z. Valiev, I.V. Aleksandrov, R.K. Islamgaliev, in G.M. Chow, N.I. Noskova (eds.), *Nanocrystalline materials: science and technology*, Kluwer, Dordrecht., 1998, p. 121.
[4] A.P. Zhilyaev, G.V. Nurislamova, B.K. Kim, M.D. Baro, J.A. Szpunar, T.G. Langdon, Acta Mater. 51 (2003) 753.
[5] M. Kawasaki, R.B. Figueiredo, T.G. Langdon, Acta Mater. 59 (2011) 308.
[6] J. Čížek, M. Janeček, O. Srba, R. Kužel, Z. Barnovská, I. Procházka, S.V. Dobatkin, Acta Materialia 59 (2011) 2322.
[7] J. Čížek, O. Melikhova, M. Janeček, O. Srba, Z. Barnovská, I. Procházka, S.V. Dobatkin, Scripta Materialia 65 (2011) 171.
[8] F. Bečvář, J. Čížek, L. Lešťák, I. Novotný, I. Procházka, F. Šebesta, Nucl. Instr. Meth. A 443 (2000) 557.
[9] J. Čížek, I. Procházka, M. Cieslar, R. Kužel, J. Kuriplach, F. Chmelík, I. Stulíková, F. Bečvář, O. Melikhova, Phys. Rev. B 65 (2002) 094106.
[10] B.T.A. McKee, S. Saimoto, A.T. Stewart, M.J. Scott, Canad.Journ. Phys. 52 (1974) 759.